REPORT DOCUMENTATION PAGE

AFRL-SR-AR-TR-04-

0627

1. AGENCY USE ONLY *(Leave blank)*	2. REPORT DATE	3. REPORT TYPE AND DATES COVERED
		01 Jul 2002 - 30 Jun 2004 FINAL

4. TITLE AND SUBTITLE
(DURIP FY02) Advanced Fabrication and Characterization of Quantum and Nanophotonic Devices and Systems

5. FUNDING NUMBERS
61103D
3484/US

6. AUTHOR(S)
Professor Fainman

7. PERFORMING ORGANIZATION NAME(S) AND ADDRESS(ES)
THE REGENTS OF THE UNIVERSITY OF CALIFORNIA SAN DIEGO
OFFICE OF CONTRACT AND GRANT ADMIN
9500 GILMAN DRIVE #0934
LA JOLLA CA 92093-0934

8. PERFORMING ORGANIZATION REPORT NUMBER

9. SPONSORING/MONITORING AGENCY NAME(S) AND ADDRESS(ES)
AFOSR/NE
4015 WILSON BLVD
SUITE 713
ARLINGTON VA 22203

10. SPONSORING/MONITORING AGENCY REPORT NUMBER
F49620-02-1-0369

11. SUPPLEMENTARY NOTES

12a. DISTRIBUTION AVAILABILITY STATEMENT
DISTRIBUTION STATEMENT A: Unlimited

12b. DISTRIBUTION CODE

13. ABSTRACT *(Maximum 200 words)*

The program completed its acquisition of equipment for the Micro- Fabrication Facility. The facility is used for fabrication of Quantum and Nanophotonic devices and consists of a CAIBE system capable of sub- micron resolution anisotropic (i.e. high aspect-ratio) etching and a RIE refumished by INTELVAC Inc. A major capability is a facility for near field complex amplitude characterization with nanoscale spatial and femtosecond scale time resolution for nanophotonics applications. This facility was designed and built in house. The necessary equipment and components to construct the sub-systems have been integrated into the system and are summarized below: (l)Femtosecond MIRA OPO, Coherent Inc. , and b) Near Field Scanning Optical Microscope (NSOM), TS2000 Nanonics Imaging Ltd. The total cost of the acquired equipment for fabrication and Characterization of Quantum and Nanophotonic Devices and Systems was $260,000. The acquired equipment during the reporting period was used to support needs of nanofabrication and characterization of several projects at UCSD: (I) "Quantum device technologies — applying 2-D photonic crystals," (Y. Fainman, L. J. Sham, C. Tu) supported by AFOSR and DARPA's Quantum Information Science and Technology Programs; (2)"Artificial Dielectrics and Photonic Crystals for STAB Elements: the Receiver" (Y. Fainman) supported by DARPA/STAB Program SPAWAR/DARPA #N66001-00-C-80'75; and (3) "Optical Nonlinearities Enhanced by Near-field Diffraction in Artificial Dielectric Nanostructures" (S. Esener- P1, Y. Fainman, Y. H. Lo, S. Bhatia) supported by DARPA's OPTOELECTRONIC TECHNOLOGY CENTER-CHIPS led by UCSD#MDA72-00-1-001 9.

14. SUBJECT TERMS	15. NUMBER OF PAGES
	16. PRICE CODE

17. SECURITY CLASSIFICATION OF REPORT	18. SECURITY CLASSIFICATION OF THIS PAGE	19. SECURITY CLASSIFICATION OF ABSTRACT	20. LIMITATION OF ABSTRACT
Unclassified	Unclassified	Unclassified	UL

Final Technical Progress Report

for AFOSR DURIP Grant on

Advanced Fabrication and Characterization of Quantum and Nanophotonic Devices and Systems

Sponsored by

Air Force Office of Scientific Research

Under Grant F-49620-02-1-0369

for Period till September 1, 2004

total: $260,000

Grantee

The Regents of the University of California, San Diego

University of California, San Diego

La Jolla, CA 92093

Principal Investigators: Y. Fainman (UCSD), (858) 534-8909

Program Manager: Dr. G. Pomrenke, (703) 696-8426

1..Acquired Equipment

1.1 **Micro-Fabrication Facility** – used for fabrication of Quantum and Nanophotonic devices is consisting of a CAIBE system capable of sub-micron resolution anisotropic (i.e. high aspect-ratio) etching. RIE refurnished by INTELVAC Inc tel. (905) 873-0166 att: Dino Deligiannis

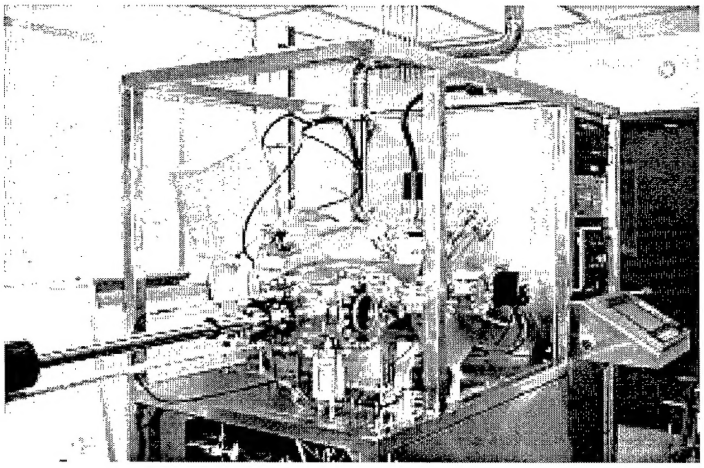

1.2 Facility for near field complex amplitude characterization with nanoscale spatial and femtosecond scale time resolution for nanophotonics applications

This facility was designed and built in house. The necessary equipment and components to construct the sub-systems which have been integrated into the system are summarized below:

a) Femtosecond MIRA OPO, Coherent Inc.
tel. (323) 857-0008 att: Cris Thalken

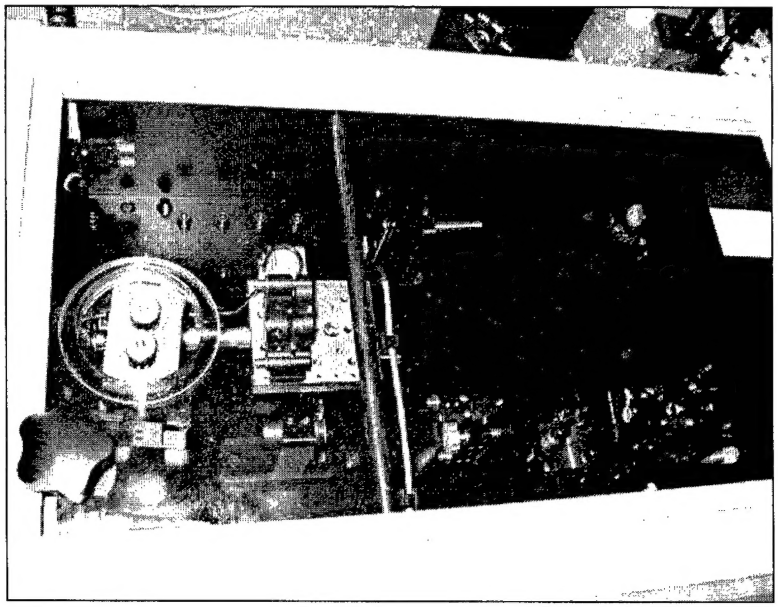

b) Near Field Scanning Optical Microscope (NSOM), TS2000
Nanonics Imaging Ltd., tel. (972) 2678-9573 Att: A. Levis

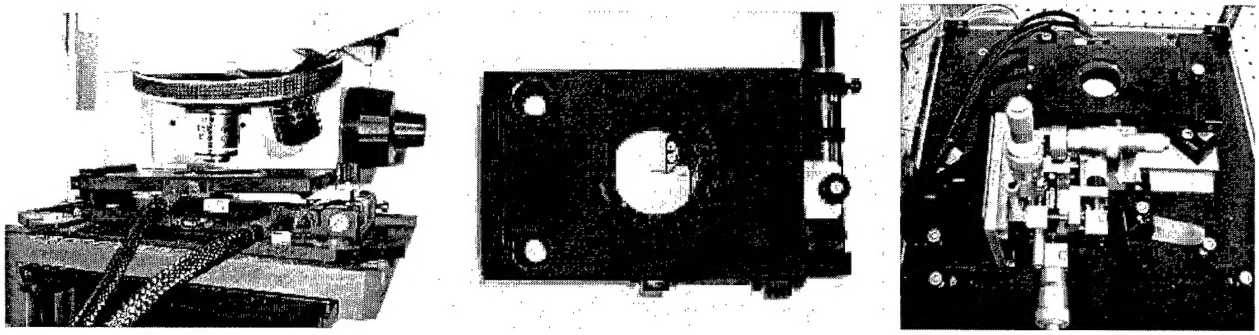

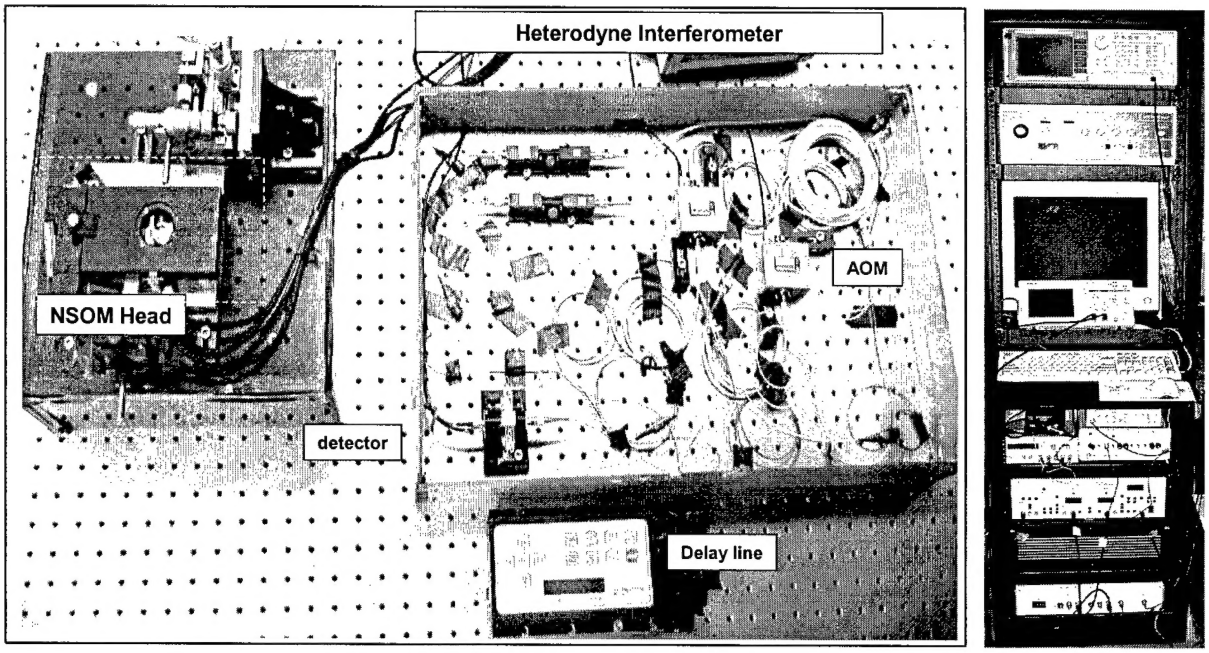

The total cost of the acquired equipment for fabrication and Characterization of Quantum and Nanophotonic Devices and Systems is $260,000.

2. Research Enabled by the Acquired Equipment

The acquired equipment during the reporting period was used to support needs of nanofabrication and characterization of several projects at UCSD:

- "Quantum device technologies – applying 2-D photonic crystals," (Y. Fainman, L. J. Sham, C. Tu) supported by AFOSR and DARPA's Quantum Information Science and Technology Programs;
- "Artificial Dielectrics and Photonic Crystals for STAB Elements: the Receiver" (Y. Fainman) supported by DARPA/STAB Program SPAWAR/DARPA #N66001-00-C-8075;
-

"Optical Nonlinearities Enhanced by Near-field Diffraction in Artificial Dielectric Nanostructures" (S. Esener- PI, Y. Fainman, Y. H. Lo, S. Bhatia) supported by DARPA's OPTOELECTRONIC TECHNOLOGY CENTER-CHIPS led by UCSD#MDA972-00-1-0019 ;

2.1 Quantum device technologies – applying 2-D photonic crystals

A. Novel Nanofabrication Technique: 3-D Holographic UV Lithography

We have developed an approach to manufacture photonic crystal-based devices based on a two-step process consisting of holographic lithography patterning to define the photonic crystal lattice followed by optical direct-write of the functional elements. First, the photonic crystal lattice is patterned in photoresist using interferometric optical lithography with multiple exposures, producing a large-area (about 1 cm^2) lithographic pattern quickly and easily. In the second step, the variations or defects in the lattice to implement the functional devices are created using optical direct-write with a strongly focused optical beam. After the patterning processes, the mask is developed and a dry-etching process (with the purchased CAIBE system) is used to transfer the desired pattern into a high dielectric constant GaAs substrate. Since the entire large-scale photonic crystal lattice is essentially created at once using interferometric patterning (Fig. 1), the direct-write process is needed only to implement the functional elements (e.g., waveguides in Fig. 2, cavities, etc.) instead of the entire lattice. Thus, this hybrid approach possesses an advantage in terms of fabrication time and cost as compared to E-beam lithography for the patterning of large-scale photonic crystal-based integrated systems.

(a) 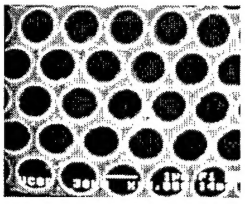 (b) 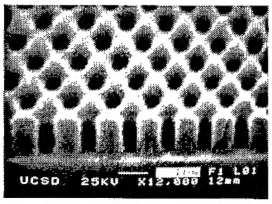

Fig. 1. Hexagonal structure lattice in resist. (a) Period: 1. 5μm diameter: 0.7μm and (b) period: 1.5μm, diameter: 1.1μm.

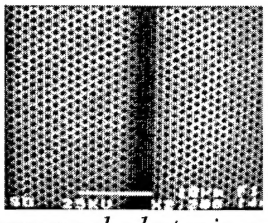 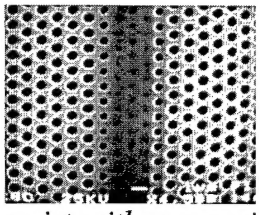

Fig. 2. 2-D photonic hexagonal photonic crystal in resist with waveguide. Three lines of holes missing waveguide in resist.

Multiple exposures were taken using an Ar^+ ion laser operating at a UV wavelength of 364nm on a UV-sensitive SU-8 negative chemically amplified photoresist. Two beams are then reflected onto the sample at an angle which can be adjusted to achieve the desired period: $\lambda/2\sin(\theta/2)$, where λ and θ are the wavelength of the laser and angle between the two beams, respectively. The in-plane substrate rotation allows for multiple exposure of the photoresist to the 1-D interference pattern, producing 2-D periodic structures, e.g. two exposures with 90^0 rotation generating square lattice, and three exposure3 with 60^0 and 120^0 rotation leading to hexagonal lattice.

The negative photoresist nature of SU-8 allows for further modification of the exposed photonic crystal lattice by selective point-by-point exposure of areas that have not yet been exposed. Such a process may be used to introduce point defects to create 2-D nanocavity, line defects to create a linear waveguide as well as any desired pattern in principle. To achieve high resolution for direct-write the line defect, we choose a reflective microscope objective lens 36X (0.52NA) with focal length of 10.4mm (from Thermo Oriel). We used vertical axis of our optical table to achieve high precision alignment by aligning the axis of the interference pattern to the translation stage axis in the translation direction.

Chemically assisted ion beam etching (CAIBE) system was used to transfer fabricated SU-8 mask into GaAs substrate (Figs. 3 and 4). With optimized dry-etching parameters, a vertical sidewall etched profile was achieved. The erosion rate of the resist and the etching rate of GaAs are 5 nm/min and 16 nm/min, respectively, such that the etching rate selectivity is approximately 3:1.

(a) 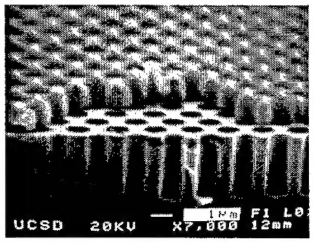

(b) 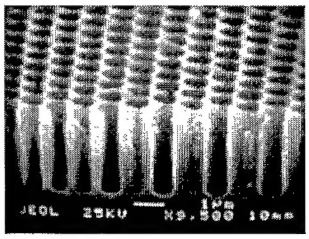

Fig. 3. Etched 2-D photonic crystal into GaAs (a) Period: 1.5μm depth: 3μm (b) Period: 1.0μm depth: 3μm

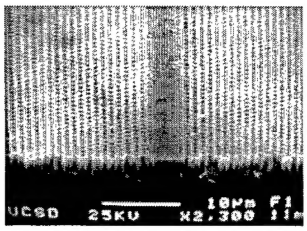

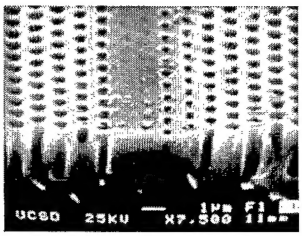

Fig. 4. Etched 2-D photonic crystal with waveguide into GaAs, period: 1.0μm, 2 line of holes cancelled waveguide depth: 2μm

We also initiated an new fabrication process of quantum dot composites. The process uses commercially available colloidal II-VI and IV-VI quantum dots and mixes them into resist for patterning to create photonic devices and circuits . This method allows us to construct photonic devices. We optimized synthesis of composite semiconductor quantum dots into resist, varying the optical photoluminescence range, density of dots as well and structure of the pattern applied to these resists (see Fig. 5): different dots and at different concentrations. An SEM of a periodic nanostructure with features of 200-300 nm made out of such a resist is shown in Fig. 6.

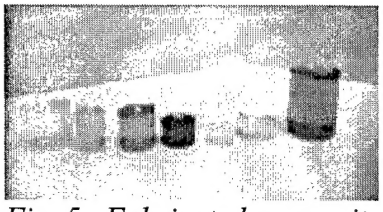

Fig. 5. Fabricated composite quantum dots in resist

We also measured the optical properties of composite materials with the embedded quantum dots (see Fig. 5). The measured the absorption and the photoluminescence (PL) of the CdSe quantum dots coated with a shell of ZnS to reduce the nonradiative recombination. Comparison of measured results for quantum dots in our resist and in Toluene solvent is shown in Fig. 7, indicating excellent performance of the quantum dots in solidified resist. We also measured the absorption as a function of concentration of the quantum dots (see Fig. 8) as well as compared the measured photoluminescence at romm temperature and at lo temperature of 10K (see Fig. 9).

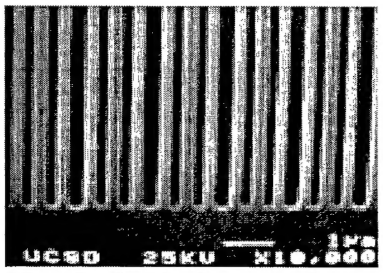

Fig. 6. SEM of a periodic structure in a quantum dot composite resist.

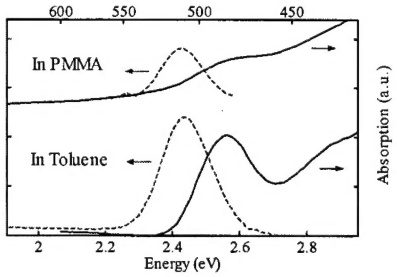

Fig. 7. Absorption and PL of the quantum dots of CdSe in solidified resist and in the Toluene solvent.

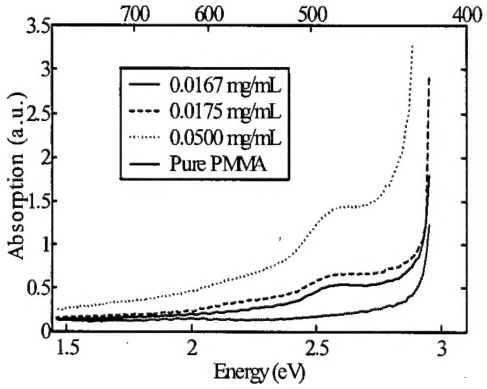

Fig. 8. Absorption of the quantum dots solidified in the resist with different concentrations.

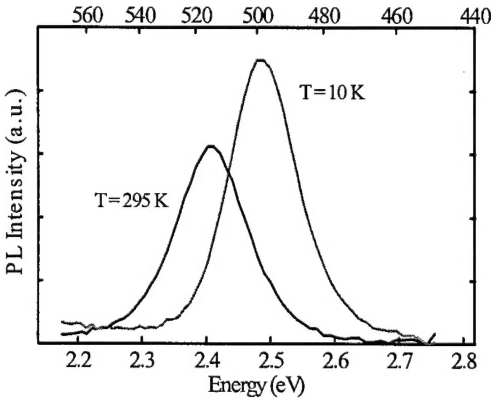

Fig. 9. PL of the solidified quantum dots in resist at room and at 10K temperatures

B. Near-field Characterization Tool for Nanophotonics

Nanofabrication uses well established microelectronics fabrication techniques, leading to the construction of fabricated nanophotonic materials and devices including form birefringent nanostructures, dispersive nanostructures, resonant photonic crystal nanostructures, photonic crystal nanostructures with defects, and quantum dot structures. Developing visualization, imaging and characterization tools for both structural and functional tests has been the least developed for nanophotonics applications due to a fundamental issue that these tools function at a wavelength that is larger than the device's geometric features making it impossible to use standard free space imaging systems (e.g., microscopes) that operate with the resolution limited by diffraction. It is also evident that for numerous nanophotonic device applications, these tools should be able to provide measured complex amplitude of the operating optical fields over a broad spectral range to allow time resolved characterization on the femtosecond resolution scale as well as full

characterization of nonlinear effects. The latter feature is of high importance for both nanoelectronic and nanophotonic device characterization and testing. The basic set-up of the coherent NSOM operating at 1.5 μm thaqt we have built is shown schematically in Fig. 10. The coherent NSOM enabling measurement of complex amplitude of the optical fields is implemented by combining a NSOM and a heterodyne interferometer.

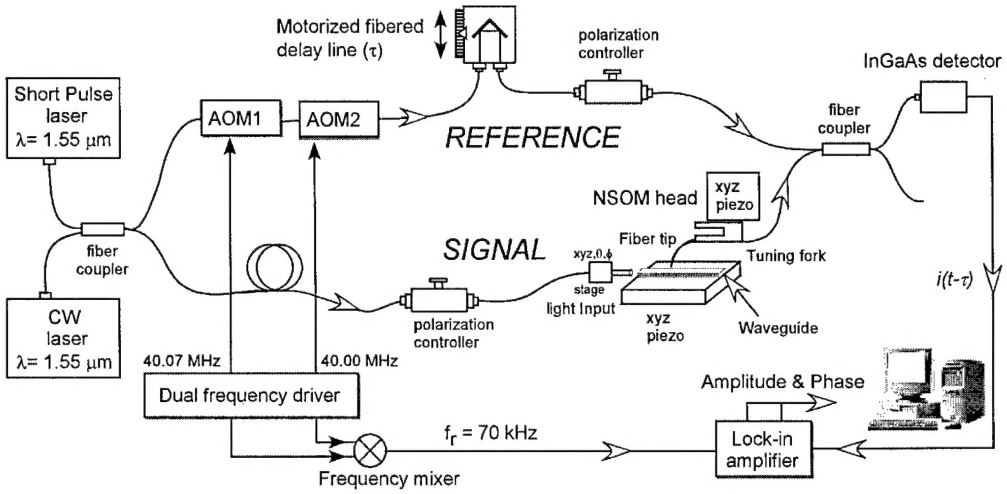

Fig. 10. Set-up of the 1.55 μm coherent Near-field Scanning Optical Microscope working either in CW or with ultra-short pulses.

The heterodyne detection is a shot noise limited detection. It offers an elegant way to increase a weak electronic signal up to a point where the shot noise dominates the thermal noise of the detector. Moreover, the heterodyne interferometer is a powerful tool for measuring the optical phase with high resolution. We built an all fiber-based system to achieve interferometric stability and to operate at a telecommunication wavelength in the near infrared range (using CW and ultra-short pulses at λ=1.55μm). The 1.55 μm laser light is split into two arms, the signal and the reference arms of a heterodyne interferometer. The light of the reference arm travels through two acousto-optic modulators and an optical delay line. The frequency is shifted using a pair of modulators operated at 40.00 MHz and 40.07 MHz, respectively. The light of the signal arm is injected into a waveguide using a 90°-cleaved bare fiber and a high-precision five-axis positioning system. A polarization controller at the reference arm is used to get the maximal contrast of the interference. Another polarization controller, placed in the signal arm, controls the input light polarization. A NSOM fiber tip is brought close to the surface using a commercial Atomic Force Microscope (AFM) which is also a Near-Field Scanning Optical Microscope (purchased *TS2000 Nanonics Imaging Ltd.*) operating in tapping-mode using a tuning fork at a resonance frequency around 32 kHz. When the tip approaches the surface, the resonance frequency changes according the Van der Waals forces between the tip and surface atoms interaction. The AFM electronic feedback can therefore control the sample-tip distance within a few nanometers. The evanescent light emerging from the waveguide is collected by the NSOM fiber tip and interfered with the optical field from the reference arm. A beat signal, due to frequency shift induced by the acousto-optic modulators, at 70 kHz is then detected by an InGas photodetector and a lock-in amplifier separates the amplitude and the phase from the output signals. The lock-in amplifier requires an electronic reference signal, at the beat frequency, which is coherent with the measured signal. The signal is demodulated at the beat frequency within a narrow bandwidth. The topography, amplitude and phase are mapped simultaneously.

For the pulsed system, we use 77MHz repetition rate pulses derived from an OPO driven by a mode locked femtosecond tunable pulsed laser (purchased *Femtosecond MIRA OPO, Coherent Inc.).* A motorized optical delay line with 2 fs resolution steps is used to overlap the ultra-short pulses (200fs to 1ps bandwidth) coming from the arms of the interferometer and thus get constructive interference. Indeed, the optical path lengths of the two arms of the interferometer have to be equal within 30 μm to get a signal. The phase accuracy, for measurement over a long time (minutes), depends strongly on the interferometer stability (mechanical, thermal and air fluctuation).

This device is an interesting and promising tool to locally probe the optical near-field of nanostructures. Thus, we believe that nanofabrication of nanophotonic devices can be considerably improved and better understood by conducting studies of near field interactions exploiting the visualization and imaging using the coherent NSOM. It is essential to first characterize our instrument with a simple structure. The waveguide core is a 5 μm by 5.3 μm doped glass (n_c= 1.56 @ 1.55μm) ridge structure, covered with a top-cladding doped glass (n_{cl}= 1.43 @ 1.55μm). Near the measuring area, a portion of the top-cladding above the waveguide (Fig. 11a and 11b) has been removed by etching process. In this case, the sample surface (above the waveguide core) has no topography and can thus avoid artifacts due to the structure. Also, the NSOM tip can also collect a bigger amount of evanescent light coming from the waveguide core.

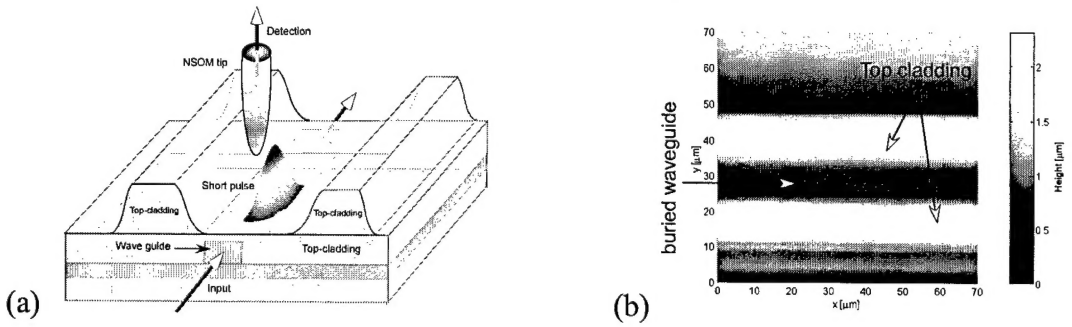

Fig. 11. Schematic diagram of the experimental structure (a) and AFM image (70 μm × 70 μm scan size) (b) of the waveguide area (top view) where a portion of the top-cladding has been partially removed.

By scanning the structure surface, the fiber tip collects evanescent light emerging from the waveguide. A signal can therefore be detected only if the cross-correlation

$$C(\tau) = \int dt\, E_{sig}(t) E^{*}_{ref}(t-\tau) \qquad (1)$$

between the two pulses (reference and signal) is non-zero. This can be obtained by varying the relative time delay τ. The measured heterodyne signal,

$$i(t-\tau) \propto \cos\left[2\pi\Delta f \cdot (t-\tau) + \varphi(t-\tau)\right], \qquad (2)$$

where Δf is the beat frequency of the signal and the reference channel which is used for lock-in detection to extract the complex amplitude information, and $\varphi(t-\tau)$ is the relative phase difference

between the signal and the reference. The amplitude (Fig. 12a) and phase (Fig.12b) are mapped by scanning the surface (for a fixed value of τ). By moving the relative position of the delay line (τ), Eq. (1) is satisfied and the temporal position of the pulse can be mapped. The amplitude is the cross-correlation function amplitude. The phase (iso-phase lines) is linear (laterally in y) as a plane wave phase. Outside of the waveguide area, the signal-to-noise ratio is zero and the phase is therefore cannot be detected. Indeed, the standard deviation of the phase depends on the inverse of the square root of the signal-to-noise ratio.

(a) 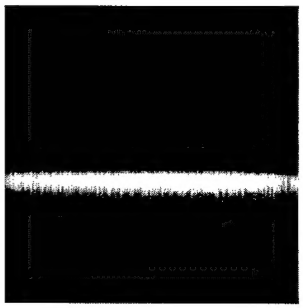 (b) 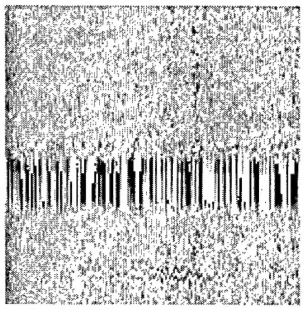

Fig. 12. Top view of the 2-d normalized amplitude (a) and phase ([$-\pi$, π]) of the evanescent field of a femtosecond short pulse mode (70 μm × 70 μm scan size) (b).

Note that the interaction of the tip with the radiation can be neglected in this specific case. Indeed, for this application, high-resolution imaging is not required because the optical field features are within the same scale as the size as the tip. Moreover, the tip scanning step, e.g. 273nm in Fig. 13b, is bigger than the tip apex size (around 100nm). If the features were much smaller, the tip-radiation interaction will need to be considered.

A cross-section of the structure topography (Atomic Force Microscope image) is shown in Fig. 13a. The bumps are the top-cladding and the "valley" is the etched cladding above (a few hundred nanometers) the buried waveguide. Figure 13b shows the short-pulse amplitude cross-section in the waveguide. The Gaussian shape intensity mode (in y-direction) is centered in the middle of the "valley" at $y_0 = 29$ μm. The intensity is zero outside the waveguide. The signal-to-noise ratio is 14dB. The longitudinal asymmetric profile (in the x-direction) of the pulse in the waveguide shows some dispersion of the short pulse (Fig. 13c). Since the scanning area of the NSOM is limited to 70μm, compressing (and compensating) the initial pulse would enable measurement of the complete pulse cross-correlation shape. In this case, a Fourier transform of the cross-correlation would bring a complete analysis of the pulse spectrum. The pulse modes can therefore be studied and will fully characterize the light propagation in the waveguide.

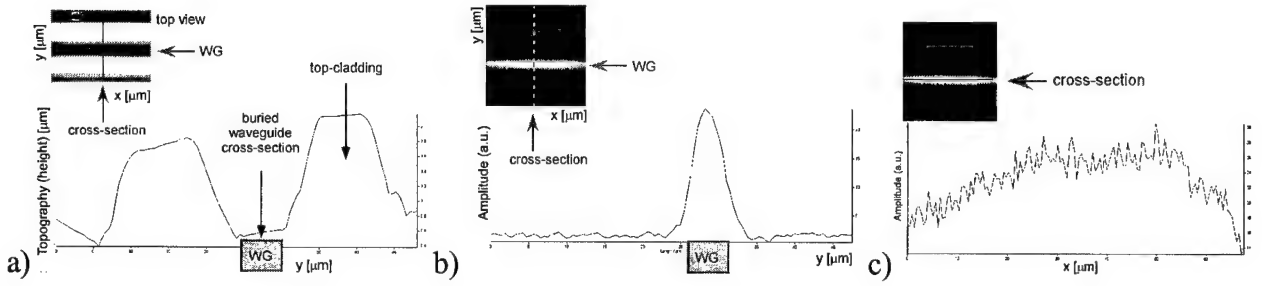

Fig. 13. 50µm cross-section (in the y-direction) of the topography (Atomic Force Microscopy) of the etched cladding above the buried waveguide (a) and cross-section of a measured evanescent amplitude of the pulse mode (b). Longitudinal profile (in the x-direction, 70µm scan size) of the pulse (c).

By varying the delay line time τ, we can track the pulse (or more precisely the cross-correlation function) at different time and spatially. If the pulse at the reference arm were a Dirac function, the correlation function $C(\tau)$ would show the envelope of the pulse in the signal arm. However, unfortunately, this can never be the case. An analysis of both pulses before their combination in the coupler would enable extrapolation of the real shape of the pulse from the measured cross-correlation function. Figure 14 shows the evolution of the "pulse envelope" in the waveguide.

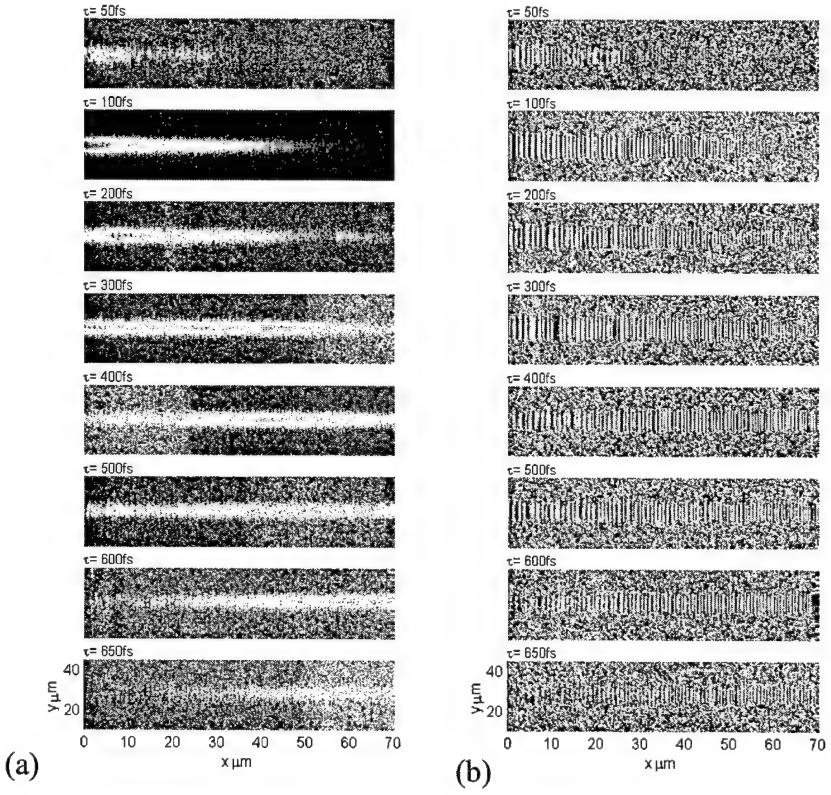

Fig. 14. Spatial (x, y) and temporal tracking of the short pulse normalized amplitude (a.u.) (a) and phase ([-π, π]) (b) in the waveguide in function of the time delay τ (from 50 fs to 650 fs).

Measurements in Fig. 14 allow the determination of the group index of the material by estimating the group velocity of the pulse. In fact, by mapping the position of the pulse maximum as a function of the time delay, we obtain the group velocity which in this case is $v_g = 2 \cdot 10^8$ *m/s*. The group index is then $n_g = 1.48$ and the theoretical value (according the Sellmeier equation) is $n_g = 1.46$. A shorter pulse and smaller steps would give better determination of this value. This technique will enable to determine the refractive index of photonic crystals and thus characterize them.

This technique also enables the characterization of local losses in photonic crystal devices and waveguides. Figure 15 shows losses that may occur in a waveguide due to some perturbations in the channel. The phase, which gives the best representation of the light propagation (k_p-*vector*), shows clearly the losses outside the waveguide (k_{loss}-*vector*) (Fig. 15b). It is important to precise that the position of the NSOM tip is very far from the waveguide entrance (about 4cm). Thus, the "spherical" wave shape is not due to some straight light coming from the input fiber light. Moreover, the initial input light direction is orthogonal to the direction of the wavefront patterns.

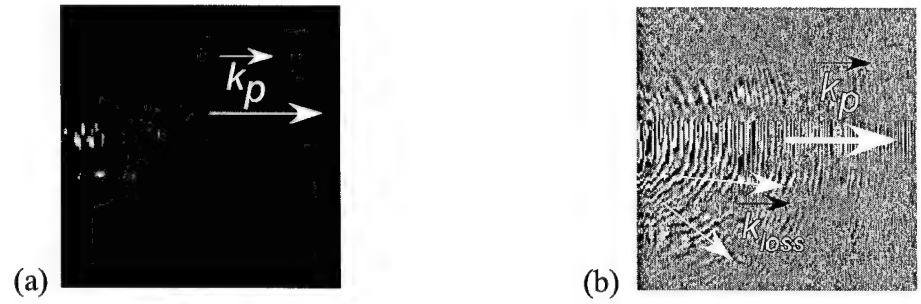

Fig. 15. Losses occurring in a waveguide. Normalized amplitude (a) and phase (b) of a half portion of a short-pulse.

From the data of Fig. 15, we can extract the intensity distribution of the guided/non-guided fields (modes) as a function of the spatial frequency (Fig.16). The algorithm for calculation of this distribution is based on finding the maximum intensity as a function of the *k*-vector (depending on the angles from -60° to 60° with 0.2°-step) while moving along the middle of the waveguide. Diagonal lines are extracted from the image matrix (Fig.15). The starting point for the line is the center of the waveguide at x = 0. If the diagonal line is not contained entirely in the waveguide, the maximum value of the line is chosen from values outside the waveguide. Otherwise, the maximum value is chosen from all values on the line. The spatial frequency is computed from the angle between the diagonal line and the x-axis and plotted vs. the normalized intensity. Figure 16a shows that most of the light is guided in the waveguide but important losses occur at the spatial frequency $k_{loss} = 0.3$ 1/μm. Figure 16b shows a comparison of the intensity distribution of the short pulse in Fig. 3, which is guided with no losses. The image accuracy of Fig. 12 is lower than that of Fig. 15, which explains the bad sampling of the function in Fig.16b.

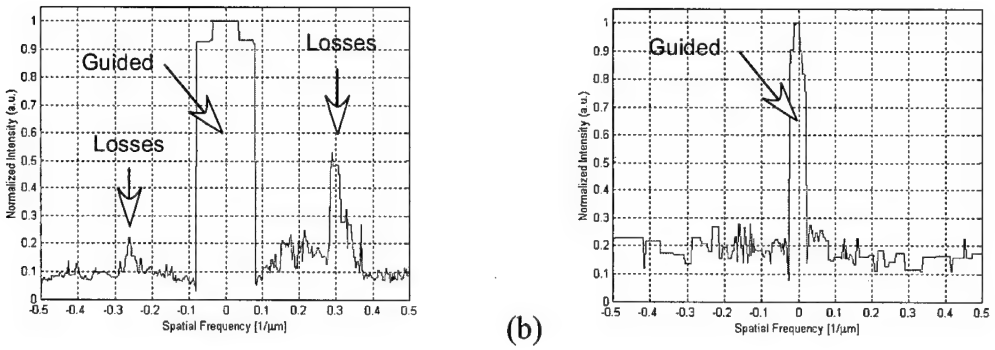

Fig. 16. Normalized intensity distribution versus spatial frequency of a short pulse (Fig. 15) traveling in a waveguide with losses (a) and another short pulse (Fig. 12) propagating with no losses (b).

By increasing the peak pulse power, non-linear effects can be investigated. In fact, the peak power can be increased up to 200 W in the waveguide, creating e.g. high-order solitons. Propagation of solitons in waveguides and photonic crystals can therefore be studied.

The investigation of near-field interactions in artificial nanostructured materials will provide a variety of functionalities useful for optical systems integration. Furthermore, near-field optical devices facilitate miniaturization and simultaneously enhance multi-functionality, greatly increasing the functional complexity per unit volume of the photonic system. Since the optical near-field of materials is controlled by the geometry, there is flexibility in the choice of constituent materials, facilitating the implementation of a wide range of devices using compatible materials for ease of fabrication and integration. In order to improve nanophotonic device performance, accurate characterization of structural and functional performance needs to be investigated simultaneously. We have developed a technique (coherent NSOM), which allows quantitative determination of the complex amplitude of the optical near-field in devices functioning at a wavelength of 1.55μm with simultaneous ability to construct the geometry with AFM accuracy. We have presented measurement of a femtosecond short pulse traveling in a waveguide introducing new capability in testing the time response of optoelectronic devices. It allows us to investigate losses that can occur in the structures (e.g. in a waveguide) and to determine the index of refraction of the material. In the future, we are planning to use this instrument for the characterization of short pulse propagation in a photonic crystal waveguide.

2.2 Artificial Dielectrics and Photonic Crystals for STAB Elements: the Receiver

Advances in the design of an integrated nanophotonic receiver consisting of a photonic crystal (PC) filter with wide angular bandwidth and narrow spectral bandwidth filter with flattop response integrated in the same volume with a PIN photodetector (PD), operated at 1550 nm region are presented in this section.

Our first step is to determine the material composition that is used to realize the resonant cavity enhanced (RCE) photodetector design. The structure of an RCE photodetector can be divided into three parts: one conventional PIN PD, and two dielectric mirrors. It is known that the InGaAs, lattice-matched to an InP substrate has excellent electric properties and can be operated around the 1550 nm spectrum. Therefore, we choose n+-doped InP, InGaAs and p+-doped InP in our PIN PD design. The

absorption coefficient of InGaAs is 10^4 /cm at 1550 nm, and the refractive indices for InP and InGaAs are 3.176 and 3.6, respectively. As for the mirrors, the alloys $In_{0.52}Ga_{0.48}As$ (3.6) and InP are chosen not only because InGaAs is lattice-matched to InP substrates, but also the refractive index ratio of InGaAs to InP is higher than other materials used for 1550 nm region.

As the second step, we design the dielectric mirrors: the mirror next to the substrate (R_2) need to have a constant reflectance in the pass band, and the mirror next to the air (R_1) with an anomalous dispersion reflectance phase relationship around the central wavelength λ_o. It is known that the 1-D photonic crystal (PC) composed of two materials will have high reflectance around λ_o as long as the optical thickness of the period is $n_1d_1+n_2d_2=\lambda_o/2$, where n_1, n_2 are the refractive indices of the two materials and d_1, d_2 are the thickness of each of the layers. Therefore, the 1-D PC can be a good candidate for the dielectric mirror R_2. On the other hand, our studies show that the characteristics required by R_1 can be achieved by constructing a multiple-mirror system. When the reflectance M_2 of the mirror next to the input medium is larger than that next to the output medium (M_1), and the thickness of the cavity C_1 is controlled to render constructive interference at λ_o, a composite mirror with an anomalous dispersion reflectance phase relationship can be realized. Therefore, our flattop-response RCE photodetector can be constructed with three mirrors and one PIN PD.

We apply the structure described above to design a photodetector that is insensitive to input incident angles. Although the shift of the reflectance band of mirrors due to different incident angles is usually inevitable, it can be reduced when the optical thickness of the high refractive index material is larger than that of the low-refractive index material. However, when the optical thickness ratio of the two materials is not equal to 1, the reflectance and the bandwidth of the mirror will be quite limited. To improve the performance of the system, we increased the number of layers for each of the mirrors to increase the reflectance and chose an optimized optical thickness ratio to ensure an adequate bandwidth. Fig. 17a shows the optimized optical thickness of each layer of the designed PD. The optical thickness ratio of high-to-low refractive indices for the mirrors is 1.2: 0.8. The total number of layers is 72 and the total thickness of the design is 8.71μm.

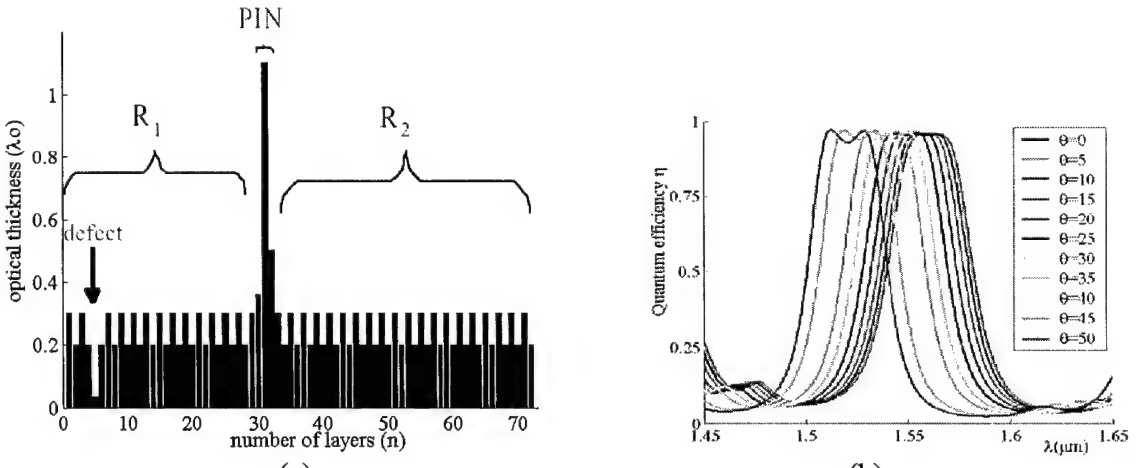

Fig. 17. (a)The optical thickness of each layer of the designed RCE PIN PD and (b) Quantum efficiency η v.s. the incident angle θ from 0° to 50°.

Fig. 17b illustrates the quantum efficiency with different incident angles. The quantum efficiency at 1550 nm is larger than 90% with the incident angle ranging from 0 to 35°, with the maximum 97.1% at

the normal incidence. The bandwidth of full wave half maximum is about 42.3 nm, and the spectrum shift is 23.1nm as the incident wave tilts from 0 to 35°.

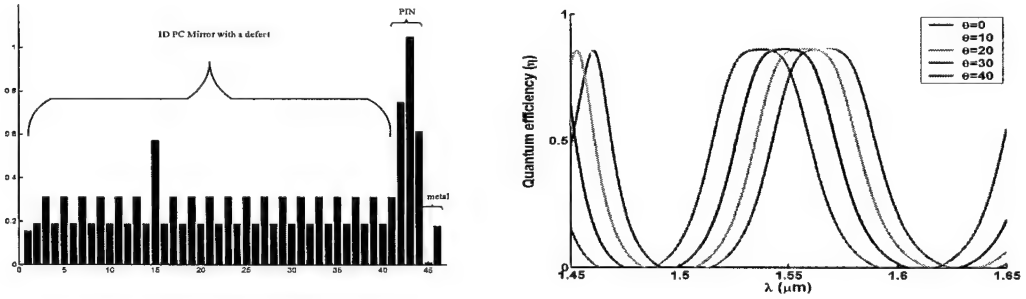

(a) (b)

Fig. 18. Resonantly enhanced photodetector with back illuminated structure: (a) design and (b) calculated quantum efficiency

The fabrication of the design of Fig. 17 may be challenging and we explore a more practical design using a folded geometry, i.e., using a metal mirror as top mirror of the resonant cavity. Such a design is summarized in Fig. 18. This design was used to fabricate a device using MBE growth followed by lithography, etching, and deposition steps. The fabricated device is shown in Fig. 19a. The fabricated devices were experimentally characterized and tested. (see Fig. 19b)

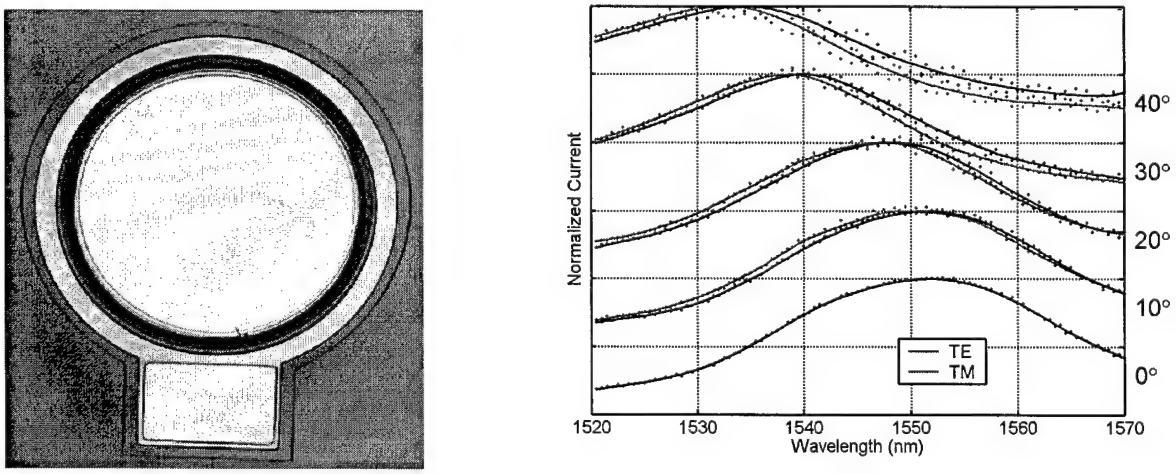

(a) (b)

Fig. 19. PC resonant receiver: (a) photograph of the device and (b) responsivity vs angle of incidence and wavelength.

2.3 Nanofabrication techniques for Nanophotonics applications: Enhanced Nonlinearities and Sensing.

We also developed novel nanofabrication techniques in solid state semiconductors with a specific focus on Nanophotonics. Nano-scale optical devices are drawing increasing interest, as their optical characteristics are promising for novel communication devices, and their compatibility with current semiconductor fabrication technology provides the possibility of miniaturized integrated optical systems. However, many of these devices require not only small feature sizes, but also deep

profiles. A common way of fabricating nano-scale features is to use electron-beam lithography. The e-beam resist itself, however, is usually not hard enough to serve as a dry-etching mask for high-aspect-ratio structures. To achieve deep, high aspect-ratio etching for nano-scale optical component fabrication, it is necessary to transfer submicron patterns from the original e-beam resist to a harder etching mask. In the following we will present the current achievements.

In this research we use SiO_2 as an etching mask for the Ar/Cl_2 Chemically Assisted Ion Beam Etching (CAIBE, *INTELVAC Inc*) process, which we use to fabricate high-aspect-ratio nanostructures in GaAs. The mask transfer procedure is illustrated in Fig. 20. First, a layer of SiO_2 is deposited on top of the GaAs substrate with Plasma Enhanced Chemical Vapor Deposition (PECVD), and a patterned layer of PMMA is created on top of the SiO_2 using E-Beam lithography. Next, we use a thermal evaporator to deposit a thin layer of Au/Cr on the surface of the sample. The patterns are then transferred onto the Cr/Au layer with a sub-micron lift-off process. Using the Au/Cr layer as an etching mask, the pattern is then transferred into the SiO_2 layer with the Reactive Ion Etching (RIE) process. This process yields a durable etch mask with the necessary profile for deep etching.

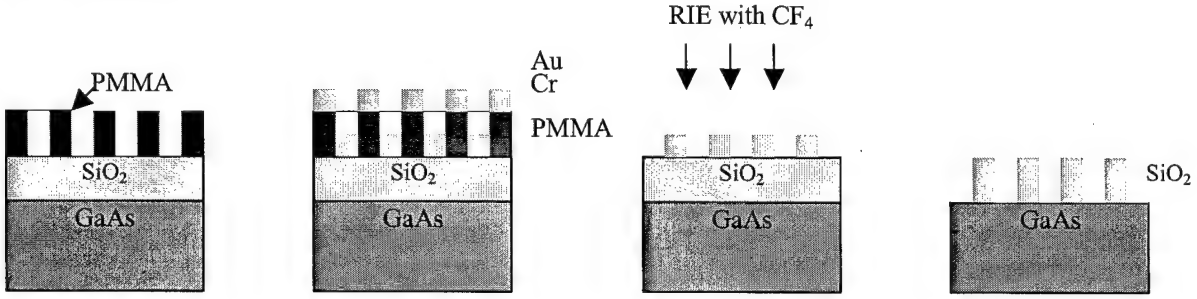

Fig. 20: Pattern transfer from PMMA into SiO_2: the pattern was transferred to a layer of Au/Cr by a lift-off process, and then carved into the SiO_2 layer with CF_4 RIE. The patterned SiO_2 layer can be used as an etching mask for CAIBE process for GaAs or similar materials.

An SEM picture of the PMMA test pattern over SiO_2/GaAs is shown in Fig. 21. Figs. 22a and 22b show two different views of the sample after the lift-off and RIE processes. The SEM pictures show a fairly good SiO_2 mask profile, which we apply next as a CAIBE etch mask for fabrication of the nanoscale high-aspect ratio optical devices.

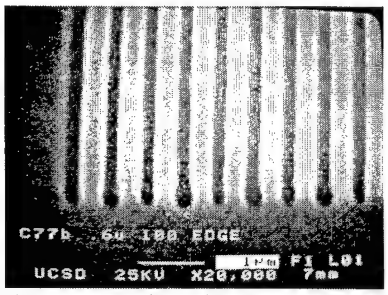

Fig. 21: SEM picture of the PMMA patterned with e-beam lithography over SiO_2 on top of a GaAs substrate with a linewidth of 0.3um.

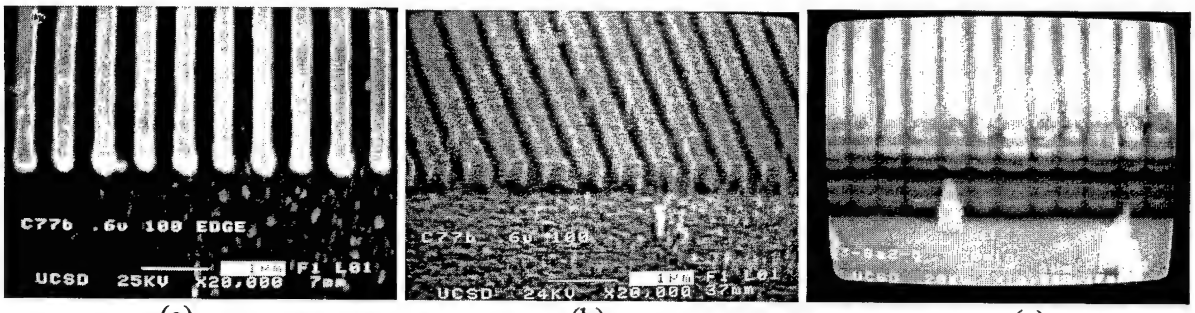

(a) (b) (c)

Fig. 22: SEM picture of the transferred pattern in SiO_2 after a lift-off process of Au/Cr and a CF_4 RIE process: (a) top view; (b) side view and (c) etched into MBE grown multiplayer structure of GaAs/AlGaAs.

The fabrication process is applicable to a variety of high-aspect-ratio nano-scale optical devices, such as photonic crystals, form birefringent materials, etc. The process was also compared to two other approaches. The result shows that a good quality lift-off can be achieved in the submicron regime and can be a workable recipe for nanostructure fabrication. A following etching result with CAIBE also shows that the transferred pattern on SiO_2 serves as a good etching mask, and a 10:1 aspect ratio is achieved with a linewidth of 0.3um. We also transferred the mask pattern into a multiplayer structure of GaAs/GaAlAs using our CAIBE system (see Fig. 22c). In general, this technique is compatible with current semiconductor fabrication processes and provides a good mask transfer quality as well.

Etch profile control studies have been also conducted with results shown in Fig. 23.

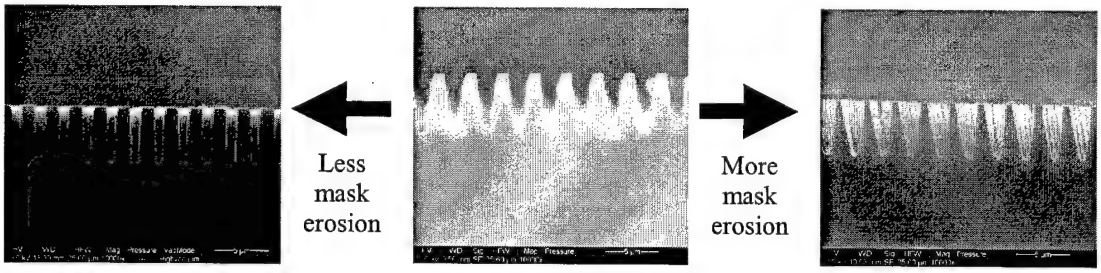

Figure 23.Nanostructure shape obtained by different level of mask erosion.

3. Publications

D. Marom, D. Panasenko, P. C. Sun, Y. Mazurenko, Y. Fainman, "Real-Time Spatial-Temporal Signal Processing with Optical Nonlinearities," IEEE Journal of Selected Topics in Quantum Electronics, v. 7, No. 4, pp. 683-693, 2002

W. Nakagawa, P. C. Sun, C. H. Chen, and Y. Fainman, "Wide field of view narrow band spectral filter base on photonic crystal nanocavities," Optics Letters, 27, pp.191-193, 2002.

W. Nakagawa, R.-C. Tyan, and Y. Fainman, "Analysis of enhanced second harmonic generation in periodic nanostructures using modified Rigorous Coupled-Wave Analysis in the undepleted pump approximation," J. Opt. Soc. Am. A, 19, 1919-1928, 2002

D.Panasenko, P.-C. Sun, N.Alic, Y.Fainman. "*Single shot sonogram generation using time gating of a spectrally decomposed ultrashort laser pulse,*" Applied Optics, 41, 5185-90, 2002.

D.Panasenko and Y.Fainman "*Interferometric correlation of infrared femtosecond pulses with two-photon conductivity in a silicon CCD,*" Applied Optics, 41, 3748-3752, 2002.

D.Panasenko and Y.Fainman, "Single-shot sonogram generation for femtosecond laser pulse diagnostics by use of two-photon absorption in a silicon CCD camera," Opt. Letters, 27, 1475-1477, 2002

G. Li; Y. Fainman, "Analysis of the wavelength-to-depth encoded interference microscopy for three-dimensional imaging," Optical Engineering, 41, 1281-1288, 2002.

D. –U. Bartch, L. Zhu; P. C. Sun, Y. Fainman, W. R. Freeman, "Retinal imaging with a low-cost micromachined membrane deformable mirror," Journal of Biomedical Optics, vol.7, (no.3), p.451-6, July 2002.

Liu Rong, TA Schmedake, Yang Li Yang, MJ Sailor, Y Fainman. Novel porous silicon vapor sensor based on polarization interferometry. Sensors & Actuators B-Chemical, vol.B87, no.1, 15 Nov. 2002, pp.58-62. Publisher: Elsevier, Switzerland.

K. S. Kim, D. Marom, L. Milstein, Y. Fainman, "Hybrid pulse position modulation/ultrashort light pulse code-division multiple-access systems I. Fundamental analysis," IEEE Transactions on commu.nications , 50, no.12, 2018-2031, 2002

R. Rokitski, P. C. Sun, Y. Fainman, " Spatio-temporal characterization of optical fiber output using ultra-short pulse spatial heterodyne imaging," Optical Memory & Neural Networks, vol.12, (no.1): 7-12, 2003

O Beom-hoan, Liu Rong, Yang Li Yang, MJ Sailor, Y Fainman. Vapor sensor realized in an ultracompact polarization interferometer built of a freestanding porous-silicon form birefringent film. IEEE Photonics Technology Letters, vol.15, no.6, June 2003, pp.834-6. Publisher: IEEE, USA.

D. Panasenko and Y. Fainman, " Single shot detection of femtosecond laser pulses using nonlinear absorption in a silicon CCD," Optical Memory & Neural Networks, vol.12, (no.1): 13-18, 2003

K. S. Kim, D. M. Marom, L. B. Milstein, and Y. Fainman, "Hybrid pulse position modulation/ultrashort light pulse code-division multiple-access systems-part II: time-space processor and modified schemes," *IEEE Trans. on Commun.*, Vol. 51, No. 7, pp. 1135-1148, 2003.

R. Rokitski and Y. Fainman, " Propagation of ultrashort pulses in multimode fiber in space and time," Optics Express, v.11, #13, pp. 1497-1500, June 2003

L. Pang, W. Nakagawa, and Y. Fainman, " Fabrication of opticsl structures using SU-8 photoresist and chemically assisted ion beam etching," Opt. Eng., vol. 42, pp. 2912-2917, 2003

L. Pang, W. Nakagawa, and Y. Fainman, " Fabrication of two-dimensional photonic crystals with controlled defects by use of multiple exposures and direct write," Applied Optics, vol. 42, pp. 5450-5456, 2003

Y. Fainman and D. M. Marom, "*Instantaneous imaging and processing of ultrafast waveforms*," to appear in *Encyclopedia of Modern Optics*, Eds. B. guenther, A. Miller, L. Bayvel, and J. Midwinter, (forthcoming in 2004).

M. P. Nezhad, K. Tetz, and Y. Fainman, "Gain assisted propagation of surface plasmon polaritons on planar metallic waveguides," Opt. Express 12, 4072-4079 (2004)

Moser C, Wenhai Liu, Fainman Y, Psaltis D. Folded shift multiplexing *Optics Letters, vol.28, no.11, 1 June 2003, pp.899-901*

C-H. Chen, K. Tetz, W. Nakagawa, and Y. Fainman, "Wide Field of View GaAs/Al_xO_y 1-D Photonic Crystal (PC) Filter," Applied Optics (in press).

U. Levy and Y. Fainman, "Dispersion properties of inhomogeneous nanostructures," J. Opt. Soc. Am. A., 21, 881-889 (2004).

U. Levy, C. H. Tsai, L. Pang and Y. Fainman, "Engineering space-variant inhomogeneous media for polarization control," Opt. Lett., 29, 1718-1720 (2004).

U. Levy, C. H. Tsai, H. C. Kim and Y. Fainman, "Design, fabrication and characterization of subwavelength computer-generated holograms for spot array generation," Accepted for publication in Opt. Express

U. Levy, M. Nezhad, H. C. Kim, C. H. Tsai, L. Pang and Y. Fainman, "Implementation of graded index medium using subwavelength structures with graded fill factor," Accepted for publication in J. Opt. Soc. Am. A.

K Campbell, A. Groisman, U. Levy, L. Pang, S.hayan Mookherjea D. Psaltis and Y. Fainman, "A microfluidic 2×2 optical switch," Accepted for publication in Applied physics letters

'R. E. Saperstein, D. Panasenko, Y. Fainman, ""Demonstration of a microwave spectrum analyzer based on time-domain optical processing in fiber" Opt. Lett. **29,** 501-503 (2004).

L.Pang, Y.-M Shen, K. Tetz and Y. Fainman, 'PMMA quantum dots composites fabricated via use of pre-polymerization', submitted to Optical express

L. Pang, M. Nezhad, U. Levy, C.-H. Tsai, and Y. Fainman, 'Form birefringence structure fabrication in GaAs by use of SU-8 as dry etching mask', submitted to Applied Optics

K. Tetz, Y. Fainman, "Excitation and Direct Imaging of Surface Plasmon Polariton Modes in a Two-dimensional Grating" submitted to Applied Physics Letters.

4. Interactions/transitions

A. Meetings, Conferences, Seminars, Proceedings

Y. Fainman, L. Sham, A. Scherer, and C. Tu, "Quantum device technologies – applying 2-D photonic crystals,Colloquium on Physics of Quantum Electronics, Snowbird, Co, January 7-10, 2002

W. Nakagawa, M. Nezhad, and Y. Fainman, "Tunable optical nanocavity based on modulation of near-field coupling between subwavelength periodic nanostructures," to be presented at IEEE Workshop on Interconnections within High Speed Digital Systems, Santa Fe, NM, May 12-15, 2002.

W. Nakagawa, G. Klemens, C.-H. Tsai, M. Nezhad, and Y. Fainman, "Eigenmode analysis of optical propagation in large-scale subwavelength periodic nanostructures," to be presented at Conference on Lasers and Electro-Optics, Long Beach, CA, May 19-24, 2002.

W. Nakagawa and Y. Fainman, "Tunable optical nanocavity based on modulation of near-field coupling between subwavelength periodic nanostructures," presented at OSA Diffractive Optics and Micro-Optics Topical Meeting, Tucson, AZ June 3-6, 2002.

W. Nakagawa, G. Klemens, A. Nesci and Y. Fainman, "Transverse optical field localization in nonlinear periodic optical nanostructures for enhanced second-harmonic generation," to be presented at 7th International Conference on Near Field Optics and Related Techniques, Rochester, NY, Aug 11-15, 2002.

D. Panasenko, R. Rokitski, D. M. Marom, Y. Mazurenko, P.-C. Sun, N. Alic and Y. Fainman. "*Nonlinear optical information processing with femtosecond pulses*", presented at 2002 SPIE AeroSense meeting, paper 4737-7 **(Invited)**

Y. Fainman, W. Nakagawa, C.-H. Chen, K. Tetz, L. Pang, and C.-H. Tsai, " Artificial Materials for Nanophotonics," presented at IEEE Workshop on Interconnections within High Speed Digital Systems, Santa Fe, NM, May 12-15, 2002. **(Invited)**

Y. Fainman, D. Panasenko, R. Rokitski, D. Marom, K. Oba, Y. Mazurenko, and P. C. Sun, "Ultrafast nonlinear optical processing using femtosecond laser pulses, presented at IQEC/LAT 2002, Moscow, June 22-28, 2002 **(Invited)**

Y. Fainman, D. Panasenko, R. Rokitski, D. Marom, Y. Mazurenko, and P. C. Sun, "Nonlinear Processing with Ultrashort Laser Pulses," presented at Photonics North Conference, Quebeck, Canada, June 2-6, 2002 **(Invited)**

D Panasenko, RI Rokitski, DM Marom, YT Mazurenko, Pang-Chen Sun, N Alic, Y Fainman. Nonlinear optical information processing with femtosecond pulses. SPIE-Int. Soc. Opt. Eng. Proceedings of SPIE - the International Society for Optical Engineering, vol.4737, 2002, pp.51-63. USA. **(Invited)**.

Y. Fainman, "Ultrafast information processing with optical nonlinearities," presented at Photonics-Asia SPIE conference, Shanghai, China, October 14-18, 2003, **(Invited)**

K Tetz, Chyong-Hua Chen, W Nakagawa, HH Wieder, Y Fainman. Design, fabrication and characterization of narrowband angularly-insensitive resonant cavity filter. LEOS 2002. 2002 IEEE/LEOS Annual Meeting Conference Proceedings. 15th Annual Meeting of the IEEE Lasers and Electro-Optics Society (Cat. No.02CH37369). IEEE. Part vol.2, 2002, pp.449-50 vol.2. Piscataway, NJ, USA

Y Fainman, W, Nakagawa C-H Tsai, C-H Chen, G Klemens. Nanophotonic materials and devices for optical system integration. LEOS 2002. 2002 IEEE/LEOS Annual Meeting Conference Proceedings. 15th Annual Meeting of the IEEE Lasers and Electro-Optics Society (Cat. No.02CH37369). IEEE. Part vol.2, 2002, pp.651-2 vol.2. Piscataway, NJ, USA **(Invited)**.

N Alic, Y Fainman. Data dependent phase coding for mitigation of intrachannel four wave mixing. 2002 IEEE/LEOS Annual Meeting Conference Proceedings. 15th Annual Meeting of the IEEE Lasers and Electro-Optics Society (Cat. No.02CH37369). IEEE. Part vol.2, 2002, pp.699-700 vol.2. Piscataway, NJ, USA

Y. Fainman, " Nanophotonic materials and devices," Photonics West, SPIE Conference, San Jose, ,January 25-29, 2003. **(Invited)**

Y. Fainman, "Ultrafast Information Processing with Optical Nonlinearities," CLEO/QELS, June 1-6, 2003, Baltimore, Maryland, **(Tutorial)**

Y. Fainman, D. Panasenko, R. Rokitski, D. Marom, K. Oba, Y. Mazurenko, and P. C. Sun, "Ultrafast Information Processing with Optical Nonlinearities," presented at Optics in Computing conference, Washington, DC, June 18-20, 2003. **(Invited)**

L. Pang, W. Nakagawa, C.-H. Tsai, and Y. Fainman, 'Fabrication of 2D photonic crystal using multiple exposures', Proc. SPIE 5181, 223 (2003)

M. P. Nezhad, C. Tsai, L. Pang, W. Nakagawa, G. Klemens, and Y. Fainman , "Form birefringent retardation plates in GaAs substrates: design, fabrication, and characterization", Proc. of SPIE, vol. 5225, Nano- and Micro-Optics for Information Systems, Louay A. Eldada, Editor, October 2003, pp. 69-77

C. H. Tsai, U. Levy, L. Pang, Y. Fainman, "Fabrication and characterization of GaAs-based space-variant inhomogeneous media for polarization control at 10.6um", Proc. SPIE, Nanoengineering:

- Fabrication, Properties, Optics, and Devices, Vol.5515, pp.142-149 (2004)R. E. Saperstein, D. Panasenko, Y. Fainman, "Demonstration of a RF-photonic spectrum analyzer using ultrafast optical pulses," in Technical Digest of 2003 Frontiers in Optics, The 87th OSA Annual Meeting and Exhibit (Omnipress, 2003), Session WII4.R. E. Saperstein, D. Panasenko, Y. Fainman, "Demonstration of a microwave spectrum analyzer using time-domain processing in optical fibers" in 2003 IEEE LEOS Annual Meeting Conference Proceedings (IEEE, Piscataway, NJ, 2003), 931-932.Y. Fainman," Ultrafast Signal Processing using optical nonlinearities," Optics in Computing, Switzerland, April 2004.**(Invited)**R. E. Saperstein, N. Alic, D. Panasenko, R. Rokitski, Y. Fainman, "Time-Domain Optical Processing using Chromatic Dispersion for Ultrashort Pulse Shaping" presented at 2004 IEEE LEOS Annual Meeting, Nov. 7-11, 2004 Rio Mar, Puerto RicoM. P. Nezhad, K. Tetz, U. Levy and Y. Fainman "Propagation of Surface Plasmon Polaritons on the Boundary of a Metal and a Gain Medium," presented at 2004 IEEE LEOS Annual Meeting, Nov. 7-11, 2004 Rio Mar, Puerto RicoK. Tetz, R. Rokitski , M. P. Nezhad , and Y. Fainman, "Excitation and Direct Imaging of Surface Plasmon Polariton Modes in the Near-Infrared," presented at 2004 IEEE LEOS Annual Meeting, Nov. 7-11, 2004 Rio Mar, Puerto RicoY. Fainman, " Nanophotonics for optoelectronic systems integration," presented at 2004 IEEE LEOS Annual Meeting, Nov. 7-11, 2004 Rio Mar, Puerto Rico **(Invited)** Y. Fainman, "Signal processing, imaging and cryptography with ultrashort laser pulses," presented at 2004 IEEE LEOS Annual Meeting, Nov. 7-11, 2004 Rio Mar, Puerto Rico **(Invited)**L. Pang, U. Levy, K. Campbell, A. Groisman, S. Mookherjea, D. Psaltis, and Y. Fainman, " A microfluidic 2x2 switch," presented at 2004 IEEE LEOS Annual Meeting, Nov. 7-11, 2004 Rio Mar, Puerto RicoN. Alic, G. Papen, and Y. Fainman, " Theoretical performance analysis of maximum likelihood sequence estimation in intensity modulated short-haul fiber optic link," presented at 2004 IEEE LEOS Annual Meeting, Nov. 7-11, 2004 Rio Mar, Puerto Rico presented at 2004 IEEE LEOS Annual Meeting, Nov. 7-11, 2004 Rio Mar, Puerto Rico **(Postdeadline paper)**

B. Consultative and advisory functions

Y. Fainman, "Real-time spatial-temporal signal processing with optical nonlinearities," Seminar, ECE Dept., UC-Davis, April 17, 2002

Y. Fainman, P. Yu, "RF spectrum analyser," OASP DARPA kick-off meeting, San Diego, California, August 7-8, 2002

Y. Fainman, STAB DARPA Review Meeting, August 13, 2002

Y. Fainman, "OptIPuter Program", NSF, Advisory Board, August 19, San Diego, 2002

Y. Fainman, L. Sham, A. Scherer, and C. Tu, "Quantum device technologies – applying 2-D photonic crystals," QuIST DARPA Review meeting, Cambridge, Massachusets, September 9-12, 2002.

Y. Fainman, "Optical CDMA", NSF workshop on optical Networks, October 21-22, 2002, Washington, DC

Y. Fainman, "Nanophotonics," DARPA Workshop on Photonic Crystals, January 22-23, 2003, San Diego, SPAWAR

Y. Fainman, " Research Directions in Photonics," ON*VECTOR Photonics Workshop-NTT, San Diego, February 3-4, 2003

Y. Fainman, "Why Optical Signal Processing?," DARPA DSRC Workshop, Washington, DC, February 20-21, 2003Y. Fainman, NSF Review Pannel on Nanophotonics, NSF, Washington, DC, April, 2003

Y. Fainman, STAB DARPA Final Report Meeting, September 24, 2003

Y. Fainman, NSF Career Review, NSF, Washington, DC, October 30-31, 2003

Y. Fainman - Guest Editor for the JOSA: B special issue on "Innovative Physical Approaches to the Temporal or Spectral Control of Optical Signals" 2002 (joint with Dr. Mossberg and Dr. Kitayama)

Y. Fainman - Guest Editor for the Journal on Optical Memory and Neural Networks special issue on "Ultrafast Optics" 2002

Y. Fainman, " Nanophotonic Materials and Devices for Optical System Integration," DARPA Topical Meeting on Optical Photonic Bandgap Research, January 22-23, 2003. **(Invited)**

Y. Fainman, " Research in Photonics," ON*VECTOR Photonics Workshop, San Diego, February 3-4, 2003**(Invited)**Y. Fainman, L. Sham, A. Scherer, and C. Tu "2-D photonic crystal nanocavities for quantum information processing," DARPA QuIST Program review, Los Angeles, June 23-25, 2003."Quantum device technologies – applying 2-D photonic crystals," DARPA QuIST PIs Review Conference, November 12-14, 2003, Fort Lauderdale, Florida

"Quantum device technologies – applying 2-D photonic crystals," DARPA QuIST PIs Review Conference, November 16-19, 2004, Scotsdasle, Arizona

5. Honors/Awards:

Y. Fainman was elected Fellow of the IEEE, January 2003.
Y. Fainman was elected Fellow of the SPIE, January 2004.